

COMPACT, ULTRA-BROADBAND COPLANAR-WAVEGUIDE BANDPASS FILTER WITH EXCELLENT STOPBAND REJECTION

S.-N. Wang and N.-W. Chen

Department of Electrical Engineering
National Central University, Taiwan
No. 300, Jungda Rd., Jhongli 320, Taiwan

Abstract—A compact, ultra-broadband coplanar-waveguide (CPW) bandpass filter (BPF) is demonstrated. The proposed CPW-BPF is essentially designed by exploiting CPW short-stub and open-stub structures. Technically, the proposed filter comprises shunt short-stub and series open-stub structures that are connected in a cascade topology. The higher and lower cutoff frequencies are mainly related to the electrical length of the shunt short stub and the series open stub, respectively. In addition, the stopband rejection is enhanced through an incorporation of CPW bandstop structures. The proposed filter design is verified through experimental demonstration. The corresponding lumped equivalent and transmission-line equivalent circuits are provided for circuit design purpose. Compared with the classical CPW-BPFs, the proposed filter is of a relatively simple and compact configuration. The demonstrated CPW-BPF has about 110% 3-dB fractional bandwidth, sharp selectivity, and great stopband rejection.

1. INTRODUCTION

Broadband wireless communication systems call for wideband bandpass filters (BPFs), particularly for systems operating in the microwave and millimeter wave regimes. Generally speaking, the microstrip filters appear to be the most common candidates for BPFs of this sort, and they have been studied thoroughly [1–3]. A general discussion of their designs and applications is provided in [4] and the references therein. In contrast, there has been relatively little work on wideband BPFs employing uniplanar coplanar-waveguide (CPW)

Corresponding author: N.-W. Chen (nwchen@ee.ncu.edu.tw).

structures. It is known that, as the operating frequency moves toward millimeter-wave frequencies, the integration of filters with other circuits via series and shunt circuit topologies appears to be inevitable. The CPW structure has been exploited for such BPF realizations.

Over the past decade, several designs have been proposed for wideband BPFs using the CPW structures [5–8]. In [5], the authors proposed a ribbon-of-brick-wall design that was realized by cascading several sections of quarter-wavelength open-ended series stub. This design achieved wide bandwidth but achieved only a slow roll-off rate at the lower passband edge. The authors of [6] demonstrated a BPF that exploited the periodic structure to reduce its size. The filter had 50% 3-dB fractional bandwidth, but the roll-off rate at the lower passband edge was again not good. Similarly, the BPF demonstrated in [7] consisted of cascaded CPW lowpass and highpass structures. The cascaded filter featured good stopband rejection, no repeated passbands, and relatively sharp skirt selectivity. However, the demonstrated 3-dB fractional bandwidth was limited to 70%. An ultra-wideband (3.1–10.6 GHz) BPF based on short-circuited CPW multiple-mode resonators was proposed in [8]. The 3-dB fractional bandwidth of the proposed CPW-BPF was about 110%. However, the roll-off at the lower passband edge was not sharp. Recently, an ultra-broadband BPF based on the cascaded configuration is proposed in [9]. The demonstrated filter had greater than 110% fractional bandwidth along with excellent selectivity, but its electrical size appeared to be relatively large.

Here, the authors aim for size reduction of the filter proposed in [9], as well as for improvement of stopband rejection. In essence, the proposed CPW-BPF is realized using the CPW bandpass structure (BPS) employed in [9] in conjunction with CPW bandstop structures. Compared with previous designs of filters of this sort, the proposed filter is relatively compact and the stopband rejection is drastically improved.

2. FILTER DESIGN AND ANALYSIS

In this Section, the theoretical design and synthesis of a compact and ultra-broadband CPW-BPF is presented. Technically, the proposed filter design essentially exploits CPW stub structures in a cascaded topology for the realization of a BPF of sharp skirt selectivity along with good out-of-band rejection. This Section is organized as follows. Section 2.1 outlines the characteristics of the CPW stub structures employed for the proposed filter design. In addition, the corresponding lumped equivalent circuits are provided. The lumped equivalent

circuits are obtained via curve fitting the simulated S -parameter data. The filter synthesis with the proposed stub structures is described in Section 2.2. Note that the commercial full-wave simulator HFSS is used for the characterization of the stub structures, as well as the filter synthesis.

2.1. CPW Stub Structures

In this sub-section, configuration and analysis of the proposed CPW stub structures exploited in the filter synthesis are presented. Specifically, Sections 2.1.1 and 2.1.2 demonstrate a folded shunt-stub structure and a series open-stub structure, respectively. Finally, the series short-stub structure for improvement on stopband performance is described in Section 2.1.3.

2.1.1. Folded CPW Shunt Short Stub

The conventional CPW shunt short stub (Fig. 1(a)), also known as a microwave resonator, is often used for BPF designs [9] and impedance matching networks. The air bridge marked with a gray rectangle is employed to suppress the propagation of the parasitic odd mode (slot-line mode). The fundamental resonance occurs when the stub is quarter wavelength in length at the corresponding resonant frequency. Owing to the distribute nature, the structure also resonates at the harmonics of the fundamental resonant frequency. Here, to reduce the vertical dimension of the stub configuration depicted in Fig. 1(a), the stub is folded in a T shape as shown in Fig. 1(b).

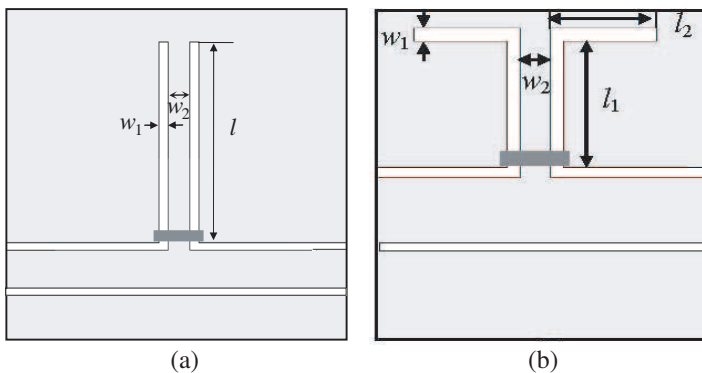


Figure 1. Schematic diagram of (a) the conventional shunt short stub and (b) the folded shunt short stub.

Figure 2 shows the S -parameter data of the straight ($l = 5.52$ mm, $w_1 = 0.4$ mm, and $w_2 = 0.85$ mm) and the folded shunt short stubs ($l_1 = 3.26$ mm, $l_2 = 2.26$ mm, $w_1 = 0.4$ mm, and $w_2 = 0.85$ mm). In Fig. 2, both structures have a fundamental resonant frequency at about 10 GHz. At the lower frequencies of the band, both structures are of similar characteristics. However, the S_{11} data are very different at the higher frequency of the band. Specifically, there is a deep drop of the S_{11} at about 14 GHz for the folded stub structure. It is shown this drop is attributed to enhancement of the radiation loss from the folded section of the stub depicted in Fig. 1(b). Indeed, the folded section essentially functions like a slot antenna at the higher frequency of the band. For verification, the radiation from the straight and folded stubs is demonstrated in Figs. 3(a) and (b), respectively. As seen in Fig. 3(b), the increase of the radiation loss is clearly observed at around 14 GHz. The radiation loss can be alleviated with an incorporation of a bandstop structure described in the Section 2.1.3 and will be addressed in the Section 3.

Figure 4 shows the corresponding lumped equivalent circuit of the folded shunt short stub. The inductor (L_1) is used to describe the characteristics of this short stub in the lower frequency regime. Hence, the lower cut-off frequency of this structure is mainly controlled by L_1 . In the higher frequency regime, a resonant circuit composed of L_2 and C_1 is used to describe its characteristics. It is shown that the higher cut-off frequency of this structure is determined by the resonant frequency of this resonant circuit.

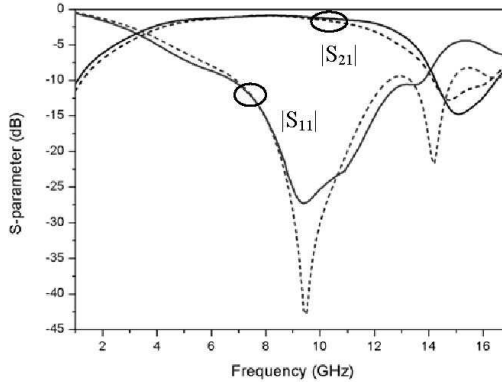


Figure 2. S -parameter data plot of the straight and folded shunt short stubs (solid-line for straight configuration and dashed-line for folded configuration).

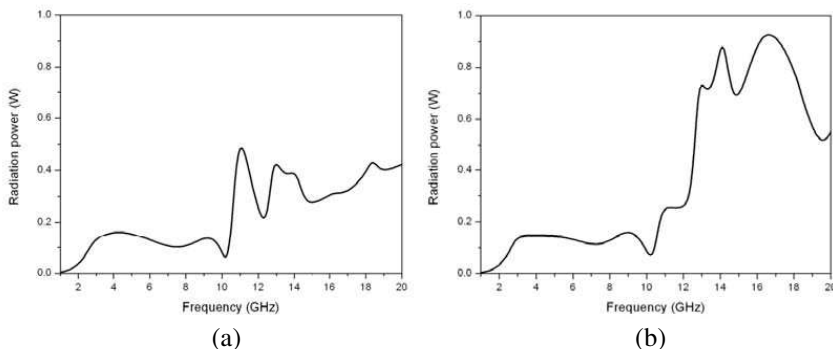


Figure 3. Radiation power from the (a) straight and (b) folded shunt short stubs.

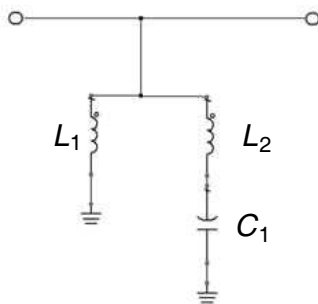


Figure 4. The lumped equivalent circuit of the CPW shunt short stub.

2.1.2. CPW Series Open Stub

In this sub-section, the characteristics of the CPW series open-stub structure shown in Fig. 5 are presented. The simulated S -parameter data of the CPW series open-stub structure ($w_1 = 0.22$ mm, $w_2 = 0.22$ mm, and $w_3 = 0.23$ mm) with different values of l are shown in Fig. 6(a). Consequently, the higher cut-off frequency of the passband decreases as l increases. On the other hand, the simulated return-loss with different values of w_3 while $w_1 = 0.23$ mm, $w_2 = 0.23$ mm, and $l = 4.83$ mm is shown in Fig. 6(b). It is shown that w_3 is a key parameter to the in-band return-loss. The corresponding lumped equivalent circuit is shown in Fig. 7. The circuit essentially comprises a resonant circuit consisted of C_1 , C_2 and L_1 and other parasitic elements. It is shown that the higher cut-off frequency is predominately

related to the resonant circuit. On the other hand, the C_3 is a key parameter to the in-band return-loss, and C_3 is mainly related to the dimension w_3 .

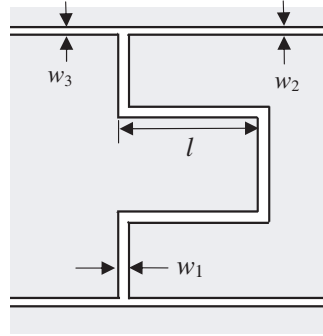


Figure 5. Schematic diagram of the CPW series open stub.

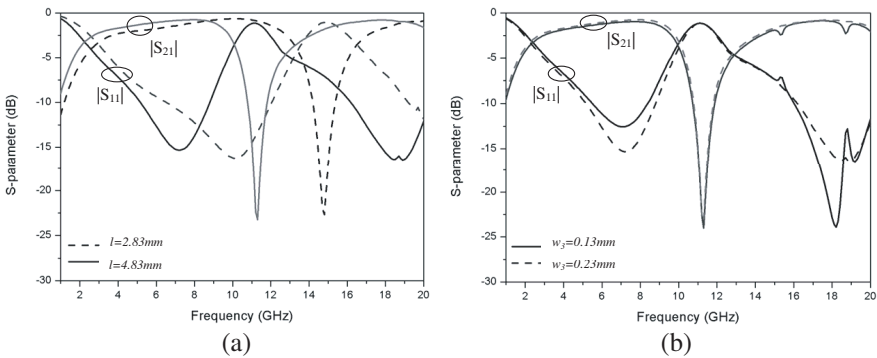


Figure 6. S -parameter data of the CPW series open stub for (a) different values of l and (b) different values of w_3 .

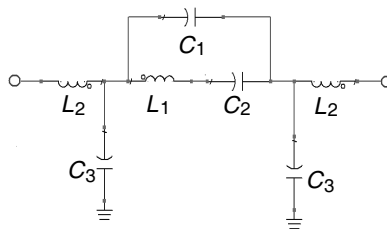


Figure 7. The lumped equivalent circuit of the CPW series open stub.

2.1.3. CPW Series Short Stub

The proposed CPW series short-stub structure for the filter synthesis is shown in Fig. 8. This structure has a similar configuration of the one demonstrated in Section 2.1.2. The simulated S -parameter data of this structure ($w_1 = 0.27$ mm, $w_2 = 0.23$ mm, and $w_3 = 0.23$ mm) with different values of l are shown in Fig. 9(a). It is shown that this stub functions like a bandstop structure. As l increases, the center frequency of the stopband decreases. On the other hand, Fig. 9(b) shows the simulated S -parameter data of this structure ($l = 1$ mm, $w_2 = 0.23$ mm, and $w_3 = 0.23$ mm) with different values of w_1 . Consequently, w_1 is associated with the fractional bandwidth (FBW) of the stopband.

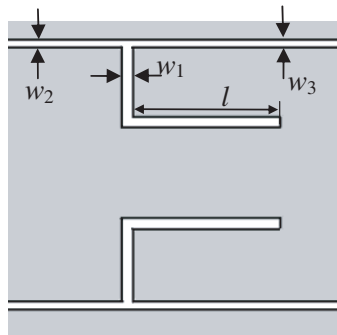


Figure 8. Schematic diagram of the CPW series short stub.

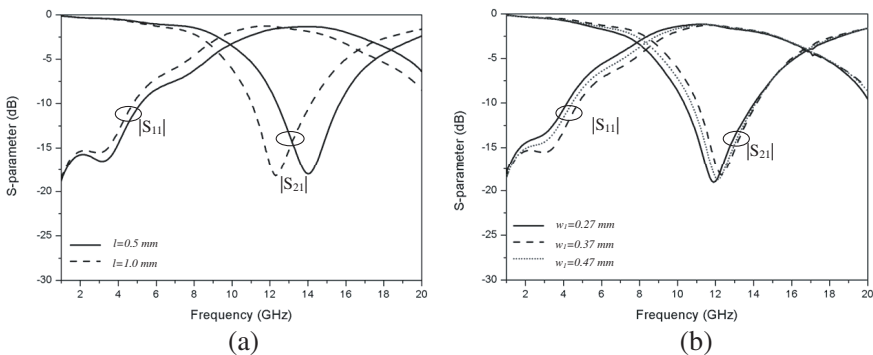


Figure 9. S -parameter data of the CPW series short stub for (a) different values of l and (b) different values of w_1 .

The corresponding lumped equivalent circuit of this stub structure is shown in Fig. 10. The circuit comprises a resonant circuit consisted of C_1 and L_1 and other parasitic elements. The resonator is used to describe the behavior of this short stub around the stopband. Specifically, the center frequency of the stopband decreases with an increase of L_1 , which is predominantly related to the dimension l . On the other hand, the stopband rejection is related to the element C_2 , which is mainly adjusted by the dimension w_2 .

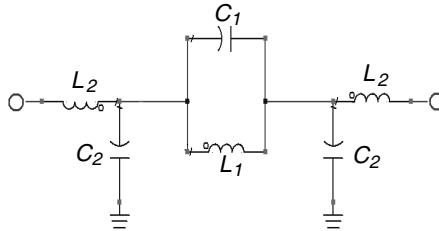


Figure 10. The lumped equivalent circuit of the CPW series short stub.

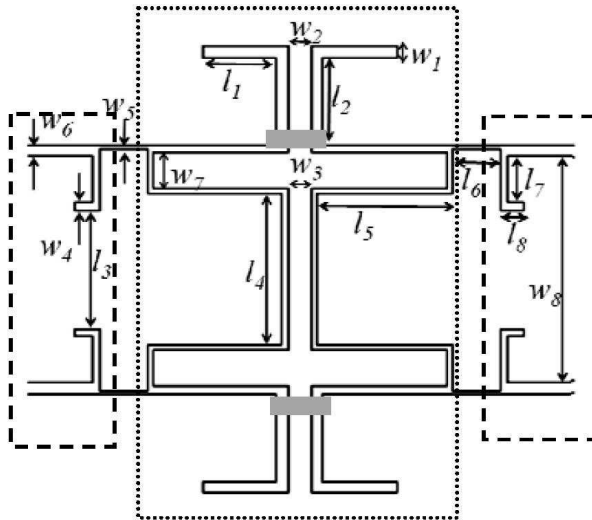


Figure 11. Configuration of the proposed CPW-BPF.

2.2. Filter Synthesis

The proposed CPW bandpass filter is realized using the three stub elements detailed in Section 2.1. The configuration of the proposed CPW-BPF is depicted in Fig. 11. The corresponding dimensions of the proposed filter are listed in Table 1. The designed filter was fabricated on an RO4350B substrate of relative permittivity 3.48, loss tangent 0.0031, and thickness 1.524 mm for the experimental demonstration. The simulation data are compared against the measurement data for verification. As demonstrated in Fig. 11, the proposed filter has three sections that are connected in a cascade topology.

First, the section outlined with a dotted line is, in essence, a cascade of the CPW series open stub described in Section 2.1.2 and the folded CPW shunt short stub presented in Section 2.1.1. Technically, the section is a design of a CPW-BPS using a series capacitor and a shunt inductor, which are realized using the CPW open and short stubs, respectively. The lower and higher cutoff frequencies of the structure are predominantly adjusted via the capacitor and inductor, respectively. In contrast to the configuration used in [9], the two short shunt CPW stubs are folded herein for a width reduction. The

Table 1. Dimensions of the proposed CPW-BPF.

w_1	w_2	w_3	w_4	w_5	w_6	w_7	w_8	Unit: mm
0.40	0.85	0.85	0.27	0.13	0.43	1.31	8.39	
l_1	l_2	l_3	l_4	l_5	l_6	l_7	l_8	
2.66	3.26	4.40	5.59	4.82	1.71	1.72	0.87	

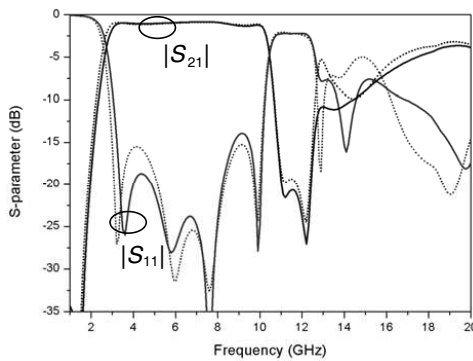


Figure 12. Simulated S -parameter data of the CPW-BPS. Solid lines: With folded shunt stubs; dashed lines: With straight shunt stubs.

simulated S -parameter data of the CPW-BPS with unfolded or folded shunt stubs are shown in Fig. 12. As a result, there is no significant difference in S -parameter data between these two cases, albeit both configurations lead to poor stopband rejection.

To improve the stopband performance of the CPW-BPS, the structure outlined with dashed lines in Fig. 11 is exploited. This structure is the CPW series short stub presented in Section 2.1.3. Here, the CPW series short stub functions as a CPW bandstop structure [10–12] of a transmission zero in the stopband of the aforementioned CPW-BPS, and the FBW of the CPW bandstop structure can be adjusted easily by the dimensions w_4 and l_3 . As mentioned in Section 2.1.3, the stopband location is attributed to the electrical length of the stub. Indeed, incorporation of structures of this sort significantly improves the stopband rejection of the CPW-BPS. As shown in Fig. 13(a), the solid lines represent the simulated results and the dotted lines are the results of the corresponding transmission-line equivalent circuit

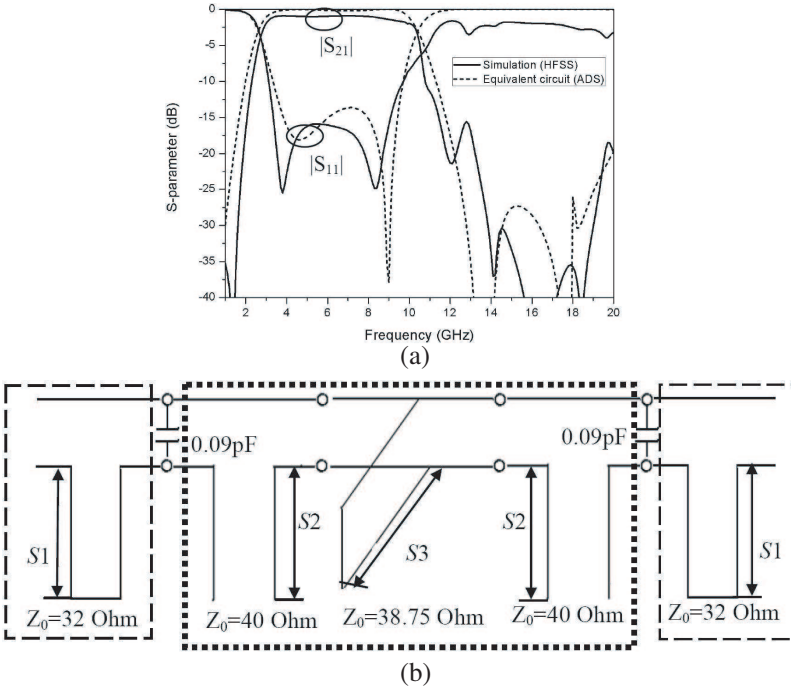


Figure 13. (a) Simulated S -parameter data of the proposed CPW-BPF. (b) Transmission-line equivalent circuit of the proposed CPW-BPF.

(Fig. 13(b)) of the proposed CPW-BPF. Note that S_1 is a quarter-wavelength at 17.8 GHz, and S_2 and S_3 are a quarter-wavelength at 6.85 GHz. The equivalent-circuit results are obtained from the circuit solver ADS. In Fig. 13(b), the lumped shunt capacitor in between the CPW-BPS and the CPW bandstop structure is mainly attributed to an increase of capacitive coupling from the small extrusion (w_5) of the interconnected section.

3. EXPERIMENTAL DEMONSTRATION

To demonstrate the effectiveness of the proposed filter design, the CPW-BPF presented in Section 2.3 is fabricated for experimental demonstration. Fig. 14 is a photograph of the fabricated CPW-BPF, which is compact, about a half-wavelength by a half-wavelength, at the center frequency (6.8 GHz) in size. The measured S -parameter data are in reasonably good agreement with the simulated values, as shown in Fig. 15. The measured 3-dB bandwidth is from 2.8 GHz to 10.1 GHz, and the fractional bandwidth is about 110%. The return loss is greater than 15 dB over the whole passband. Furthermore, sharp selectivity at both edges together with excellent stopband rejection in the entire passband is observed. Also, as shown in Fig. 16, the proposed filter also has good linearity with flat group delay variation from 0.3 ns to 0.6 ns in the passband. Indeed, as compared with the recent wideband/ultra-wideband CPW filter designs (Table 2), the proposed CPW-BPF is relatively compact and features very good selectivity and great stopband rejection.

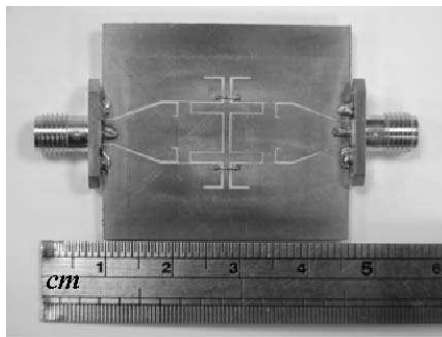


Figure 14. A photograph of the proposed CPW-BPF.

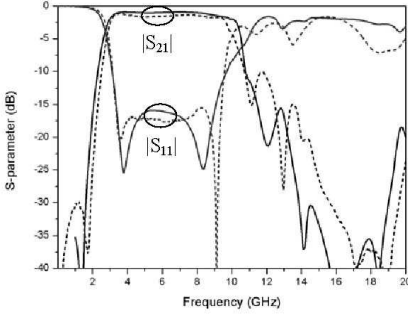


Figure 15. Simulated S -parameter of the proposed CPW-BPF (solid-line for simulation and dashed-line for measurement).

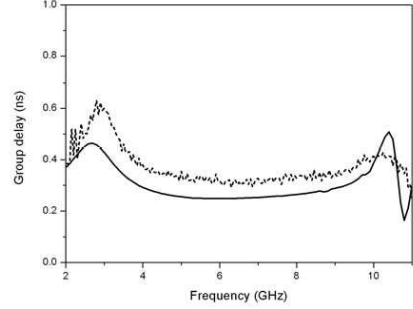


Figure 16. Group delay of the proposed CPW-BPF (solid-line: Simulation; dashed-line: Measurement).

Table 2. Comparison of the proposed CPW-BPF with the recent designs.

	FBW	Selectivity	Stopband rejection	Electrical size	Group delay variation
This work	116%	Very good	> 20 dB over the entire stopband	0.5λ	0.30 ns
[8]	116%	Poor at lower edge	N/A	λ	0.35 ns
[9]	120%	Very good	> 10 dB over the entire stopband	λ	0.36 ns
[7]	70%	Good	> 15 dB over the entire stopband	0.6λ	N/A

4. CONCLUSION

In conclusion, a compact, ultra-broadband CPW-BPF is demonstrated. The proposed CPW-BPF was designed using simple CPW-BPS and CPW bandstop structures. The demonstrated CPW-BPF features greater than 110% 3-dB fractional bandwidth, sharp skirt selectivity, good stopband rejection, and no repeated passbands. Indeed,

the sharp skirt selectivity and good stopband rejection are required to ensure a good rejection of unwanted frequencies in the vicinity of the signal frequencies. The proposed BPF is expected to find applications in wideband/ultra-wideband communication systems, uniplanar monolithic integrated circuits, and monolithic microwave integrated circuits.

REFERENCES

1. Chen, H. and Y. Zhang, "A novel and compact UWB bandpass filter using microstrip fork-form resonators," *Progress In Electromagnetics Research*, PIER 77, 273–280, 2007.
2. Razalli, M. S., A. Ismail, M. A. Mahdi, and M. N. Bin Hamidon, "Novel compact microstrip ultra-wideband filter utilizing short-circuited stubs with less vias," *Progress In Electromagnetics Research*, PIER 88, 91–104, 2008.
3. Razalli, M. S., A. Ismail, M. A. Mahdi, and M. N. Bin Hamidon, "Novel compact "via-less" ultra-wide band filter utilizing capacitive microstrip patch," *Progress In Electromagnetics Research*, PIER 91, 213–227, 2009.
4. Hong, J.-S. and M. J. Lancaster, *Microstrip Filters for RF/Microwave Applications*, Wiley, New York, 2001.
5. Lin, F. L., C. W. Chiu, and R. B. Wu, "Coplanar waveguide bandpass filter — A ribbon-of-brick-wall design," *IEEE Trans. Microw. Theory Tech.*, Vol. 47, 1589–1596, Jul. 1995.
6. Kuo, Y.-K., C.-H. Wang, and C. H. Chen, "Novel reduced-size coplanar-waveguide bandpass filters," *IEEE Microw. Wireless Compon. Lett.*, Vol. 11, No. 2, 65–67, Feb. 2001.
7. Lin, Y.-S., W.-C. Ku, C.-H. Wang, and C. H. Chen, "Wideband coplanar-waveguide bandpass filters with good stopband rejection," *IEEE Microw. Wireless Compon. Lett.*, Vol. 14, No. 9, 422–424, 2004.
8. Gao, J., L. Zhu, W. Menzel, and F. Bogelsack, "Short-circuited CPW multiple-mode resonator for ultra-wideband (UWB) bandpass filter," *IEEE Microw. Wireless Compon. Lett.*, Vol. 16, No. 3, 104–106, Mar. 2006.
9. Chen, N.-W. and K.-C. Fang, "An ultra-broadband coplanar waveguide bandpass filter with sharp skirt selectivity," *IEEE Microw. and Wireless Compon. Lett.*, Vol. 17., No. 2, 124–126, Feb. 2007.
10. Dib, N. I., L. P. B. Katehi, G. E. Ponchak, and R. N. Simons, "Theoretical and experimental characterization of coplanar

- waveguide discontinuities 49–53 for filter applications,” *IEEE Trans. Microw. Theory Tech.*, Vol. 39, 873–881, May 1991.
11. Simons, R. N., *Coplanar Waveguide Circuits, Components, and Systems*, Wiley Interscience, 2001.
 12. Liu, A. Q., A. B. Yu, and Q. X. Zhang, “Broad-band band-pass and band-stop filters with sharp cut-off frequencies based on series CPW stubs,” *IEEE MTT-S Int. Microwave Symp. Digest*, 353–356, Jun. 2006.